# Electrostatic trapping of single conducting nanoparticles between nanoelectrodes

A. Bezryadin[a] and C. Dekker[b]
*Department of Applied Physics and DIMES, Delft University of Technology, 2628 CJ Delft, The Netherlands*

G. Schmid
*Institut für Anorganische Chemie FB 8, Universität-GH Essen, 45117 Essen, Germany*

(Received 4 June 1997; accepted for publication 8 July 1997)

For molecular electronics, one needs the ability to electrically address a single conducting molecule. We report on the fabrication of stable Pt electrodes with a spacing down to 4 nm and demonstrate a new deposition technique, i.e., electrostatic trapping, which can be used to bridge the electrodes in a *controlled* way with a *single* conducting nanoparticle such as a conjugated or metal–cluster molecule. In electrostatic trapping, nanoparticles are polarized by an applied electric field and are attracted to the gap between the electrodes where the field is maximum. The feasibility of electrostatic trapping is demonstrated for Pd colloids. Transport measurements on a single Pd nanoparticle show single electron tunneling coexisting with tunnel-barrier suppression. © *1997 American Institute of Physics.* [S0003-6951(97)03235-X]

Electrical transport through mesoscopic conductors has been a major research area in the past decade.[1] Now the focus is starting to shift from artificially fabricated structures that have a minimum size set by the limits of lithography techniques to ''natural'' nm-size objects such as clusters and molecules.[2–9] A variety of ultrasmall and ultrafast electronic devices has been envisioned on the basis of single conducting molecules.[3] Electron transport through molecular wires may involve novel phenomena that have no counterpart in inorganic structures.[4] The pivotal difficulty in such molecular electronics is to attach electrical contacts specifically to single molecules. Typical dimensions ($\leqslant 5$ nm) of rigid conjugated oligomers[5] or well-defined metal clusters[6] are well below the resolution limits of electron-beam lithography ($\sim 20$ nm). There have, therefore, been few experiments on single nanoparticles reported to date. Recently, a few attempts have addressed the experimental goal of obtaining a single conducting nanoparticle between two stable electrodes. Ralph *et al.* used a vertical electrode layout to measure on nm-size Al grains.[7] Klein and McEuen used planar electrodes that were bridged with metal colloid particles using the self-assembling properties of dithiol molecules.[8] Break junctions have been used to measure transport through conjugated benzene-1,4-dithiol molecules.[9] In these first experiments deposition of the nanoparticles was poorly controlled. Typically, many particles were randomly deposited with the hope of obtaining a favorable configuration.

Here we develop a new technique, viz., electrostatic trapping (ET), that allows for *controlled* deposition of a *single* nanoparticle between two metal electrodes. This is corroborated by transport experiments on a single Pd nanocrystal at 4.2 K. The ET method is based on the attraction of polarized particles to the point of the strongest electric field (Fig. 1). If the electrodes are immersed into a liquid solvent, the dissolved particles (molecules, metal clusters) can diffuse close to the electrodes. Upon applying a voltage ($V$) one will polarize conducting particles in the vicinity of the electrodes. Due to the field gradient near the nm-size gap the polarized particles will be attracted to the region between the electrodes, in the same way as any dipole is attracted to the field maximum. The negatively charged side of the particle will be attached to the positive electrode and the positive side to the negative electrode. As a result the electrodes will be bridged with a particle if the distance between them is smaller than the particle size. The spacing between electrodes can be reduced down to 4 nm (see below). A self-limiting system which traps only a *single* particle rather than a few is possible. For this one needs to include a high resistor ($R_s$) in series with the electrodes. After trapping a single particle a current will flow between the electrodes. If $R_s$ is sufficiently high, the main part of the voltage will then drop across the resistor. Therefore the electric field in the gap will be strongly reduced, which prevents trapping of a second particle.

The sample layout is illustrated in Fig. 1. A 1 $\mu$m $SiO_2$ film is thermally grown on a Si wafer. A 60 nm low-stress

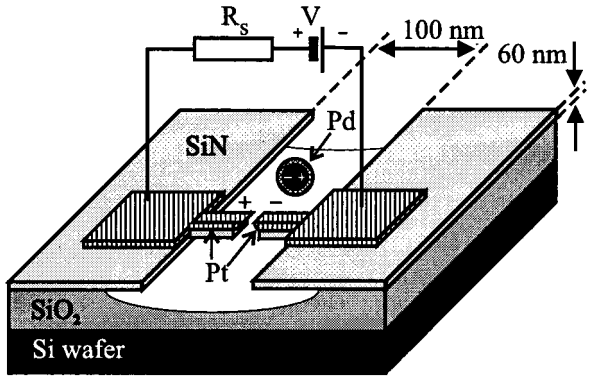


FIG. 1. Schematic representation of the sample. Pt denotes two free-standing Pt electrodes (dashed region). A ligand-stabilized Pd cluster is polarized by the applied voltage and attracted to the gap between the Pt electrodes.

[a]Electronic mail: bezryadi@qt.tn.tudelft.nl
[b]Electronic mail: dekker@sg.tn.tudelft.nl

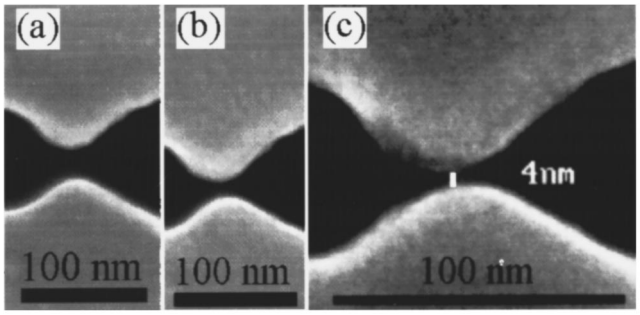


FIG. 2. SEM images of the gap between two Pt electrodes lying on SiN free-standing ''fingers'' (cf. Fig. 1). By additional sputtering of Pt on top of the electrodes, the distance between them is reduced from 25 nm in (a), to 15 nm in (b), and to 4 nm in (c). Note that the sputtered Pt film has a very smooth edge even at the nm scale.

SiN film is deposited on top. Electron-beam lithography with PMMA and reactive ion etching (with $CHF_3$) is used to open a long ($\sim$1 mm) narrow ($\sim$100 nm) slit in the SiN film with a local constriction with 20 nm spacing. $SiO_2$ is underetched in HF, which results in two free-standing SiN ''fingers'' at the constriction; these fingers are separated by a gap of only 20 nm. Next we sputter through a shadow mask a $\sim$20-$\mu$m-wide strip of Pt (usually tens of nm thick) across the slit onto the fingers. As a result we get two metal electrodes separated by a gap of $\sim$20 nm which can be reduced down to 4 nm or less by sputtering additional layers of Pt as shown in Fig. 2. All images are obtained with a Hitachi S-900 scanning electron microscope (SEM). During Pt deposition the fingers become thicker in all directions and accordingly the spacing between them slowly decreases. A few steps of imaging and subsequent sputtering are usually necessary to tune the gap down to few nanometers. Note that this approach enables for the first time the fabrication of stable metal electrodes separated by a distance that is smaller than the length of existing conducting molecules.[5] The resistance between such electrodes is very high ($\sim 10^{13}\ \Omega$ at a 5 V bias at room temperature).

To test the ET principle we have studied Pd colloids.[6] These $\sim$20 nm metal particles are covered with a monolayer of ligands ($H_2N$–$C_6H_4$–$SO_3Na$–) which prevents coalescence and makes the particles solvable in water. ET is carried out by putting a drop of water with solved particles on the electrodes, and applying a voltage of 4.5 V for a few seconds (with $R_s = 100\ \mathrm{M}\Omega$). Then we reduce the voltage and dry the sample with a $N_2$ gas flow. After the ET the sample resistance is usually reduced by two or three orders of magnitude, but *only* if there are particles in the water and if a voltage was applied. SEM shows that a single or a few nanoparticles reproducibly bridge the electrodes after ET. Figure 3(a) shows two Pt electrodes with a gap of $\approx$14 nm before the ET. In Fig. 3(b) one can see the same electrodes after the ET. ET has resulted in the deposition of a single $\approx$17 nm Pd particle that touches both electrodes. The number of trapped particles is determined by the gap size. An example where the distance between the Pt fingers ($\approx$26 nm) was larger than the particle size is shown in Fig. 3(c). As a result three particles are bridging the electrodes. The electrostatic trapping energy can be estimated as $W = [(C_p - C_g)V^2]/2$ where $C_g$ ($C_p$) is the capacitance between the electrodes without (with) the trapped particle. Since in our case $C_p \gg C_g$ and $e/C_p \sim 0.15$ V (see below), we obtain $W \approx (C_p V^2)/2 \sim 3$ eV at $V = 1$ V. This is two orders of magnitude higher than the thermal energy at room temperature ($k_B T \approx 0.03$ eV).

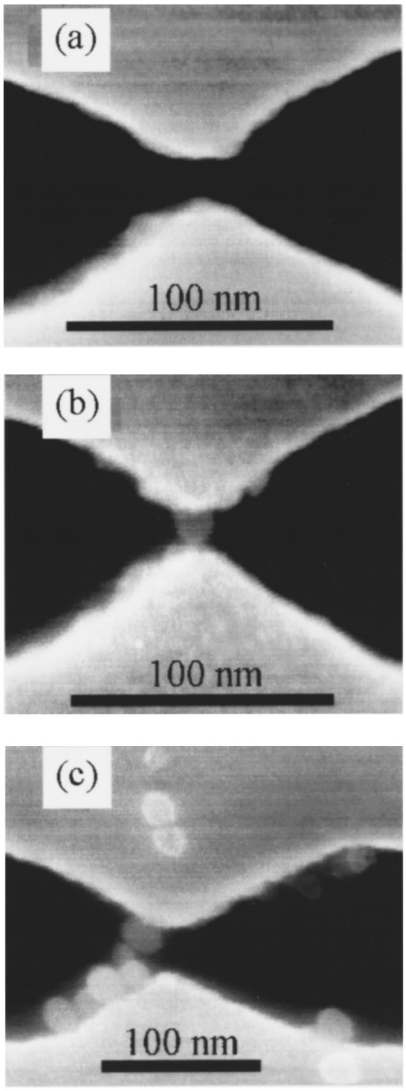


FIG. 3. (a) Pt electrodes (white) separated by a $\approx$14 nm gap. (b) After ET, the same electrodes are bridged by a single $\approx$17 nm Pd particle. (c) Another example where three Pd colloids are trapped across a $\approx$26 nm gap.

The single Pd particle junctions produced by ET were sufficiently stable to allow the study of their transport properties. The low-temperature transport involves single electron tunneling, as expected for the double-barrier system formed by the Pd cluster separated from the two leads by ligand barriers. Typical current–voltage ($I$–$V$) curves measured on a sample similar to Fig. 3(b) are shown in Fig. 4. At $T = 4.2$ K the most pronounced feature is the Coulomb gap. The gap voltage is $V_c \approx 55$ mV. This is one order of magnitude higher than is usually observed in artificial double-barrier systems. At $V < V_c$ current is blocked because of the low capacitance ($C_\Sigma$) of the Pd cluster which leads to the high charging energy $E_c = e^2/2C_\Sigma$ that is required for putting an extra electron on the nanoparticle. A rough estimate for $C_\Sigma$ is given by the self-capacitance $C_s = 4\pi\epsilon_0 r = 9.4 \times 10^{-19}$ F of the spherical ($2r \approx 17$ nm) particle. This yields

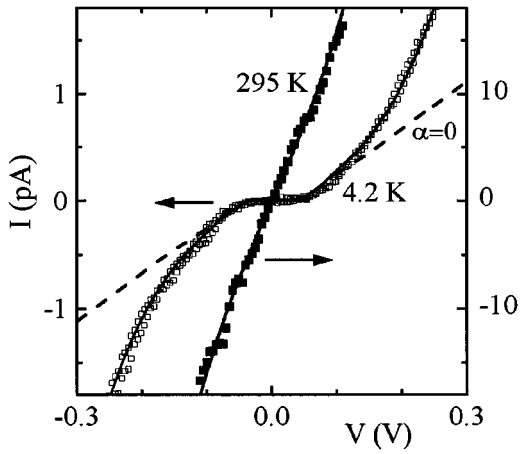


FIG. 4. Current–voltage curves measured at 4.2 K (open squares) and at 295 K (solid squares). The solid curves denote fits of the KN model. Fitting parameters for these curves are $V_c=55$ mV, $R_0=1.1\times10^{11}\ \Omega$, $q_0=0.15e$ (offset charge), and $\alpha=E_c\tau/\hbar=0.5$. The dashed curve ($\alpha=0$) represents the conventional model which assumes a voltage–independent tunnel barrier.

$V_c=e/C_s\approx170$ mV. The experimental value is lower because the total capacitance ($C_\Sigma\approx C_s+C_e$) of the particle also includes the capacitance to the electrodes ($C_e\approx2C_p$) which here is comparable to $C_s$. At $V>V_c$ the $I-V$ curve is not linear, as is usually observed. Instead, an exponential increase of the current is found at 4.2 K. This can be explained by suppression of the effective tunnel barrier by the applied voltage.

The coexistence of single electron tunneling and barrier suppression was, to our knowledge, not experimentally observed before. This new regime was, however, analyzed theoretically by Korotkov and Nazarov (KN).[10] They approximate the $I-V$ curve of each tunnel junction by the Stratton formula[11] $I(V)=(2\pi k_BT/eR_0)[\sinh(eV\tau/\hbar)/\sin(2\pi\tau k_BT/\hbar)]$ in which $\tau=L/\sqrt{2U/m}$ is the tunneling traversal time, $U$ is the tunnel barrier height, $L$ is the barrier width, $T$ is the temperature, $R_0$ is the junction resistance at zero bias and $T=0$, $m$ is the electron mass, and $\hbar$ is Planck's constant. At 4.2 K the fitting curve (solid curve through open squares in Fig. 4) calculated using the KN model is in good agreement with the measurements. Exponential $I-V$ curves are predicted if the nonlinearity parameter $\alpha\equiv E_c\tau/\hbar$ is of order unity or higher. This parameter $\alpha$ is defined as the ratio between the charging energy $E_c=eV_c/2$ and the characteristic energy $\hbar/\tau$ for which barrier suppression occurs. From the fit we obtain $\alpha=0.5$, consistent with the exponential $I-V$ curves observed in the experiment. By contrast, the dashed curve calculated assuming a voltage-independent tunnel barrier ($\alpha=0$) does not fit the data at all. It is quite remarkable that the room-temperature $I-V$ curve calculated using the *same* fitting parameters is also in good agreement with the experimental data (solid line through the filled squares in Fig. 4). This demonstrates a good temperature stability of our single particle device. It also indicates the applicability of the KN model which confirms, among other things, the tunnel character of the charge transport through the ligands. From the fitting parameters $\alpha$, $V_c$, and $R_0=R^*\exp(2L\sqrt{2mU}/\hbar)$ one can estimate the order of magnitude of the width ($L$) and the height ($U$) of the tunnel barrier as well as the tunneling traversal time $\tau$. The constant $R^*$ can be approximated by the quantum resistance (13 k$\Omega$) divided by the number of quantum channels participating in the tunneling. This number ($\sim10$) is of the same order of magnitude as the ratio of the contact area ($\sim1$ nm)$^2$ and half of the Fermi wavelength ($\sim0.3$ nm)$^2$. From the above equations one obtains $U=eV_c\ln(R_0/R^*)/8\alpha\approx0.25$ eV, $L=\hbar\sqrt{\alpha\ln(R_0/R^*)/emV_c}\approx3.4$ nm and $\tau=2\alpha\hbar/eV_c=1.3\times10^{-14}$ s. These values are physically plausible. The value for $L$, however, is a few times larger than the thickness of the organic shell ($\sim1$ nm). Agreement can be achieved if we assume a high electron effective mass inside the ligand barrier ($m^*\sim10\,m$), which may indicate polaronic effects.

The ET technique is very general. It can be used with polarizable nanoparticles of any type. We have, for example, also tested it successfully on micron-long carbon nanotubes[12] as well as on 5-nm-long conjugated molecules of dodecathiophene.[5] Here, real-time monitoring of the ET is possible. To trap a dodecathiophene oligomer we use electrodes separated by a 4 nm gap [cf. Fig. 2(c)] that are immersed into an insulating organic solvent (toluene). At $V=3$ V only a weak ($\sim3$ pA) leakage current is detected in clean toluene. Upon slowly increasing the concentration of molecules in the solvent no change is observed in the current. After a waiting period ($\sim100$ s), however, a sudden increase of the current to a $\sim1$ nA level is detected which indicates the trapping of a single molecule. ET thus allows the controlled deposition of a variety of nanoparticles. This in turn opens the way to explore the transport properties of single molecules and clusters.

The authors thank E. W. J. M. van der Drift, E. J. G. Goudena, L. de Jongh, L. P. Kouwenhoven, Yu. Nazarov, P. M. Sarro, S. J. Tans, and Ya. Volokitin, for useful discussions, and A. Korotkov for supplying the program for numerical calculations. This research was funded by the Stichting voor Fundamenteel Onderzoek der Materie (FOM).

[1] C. W. J. Beenakker and H. van Houten, Solid State Phys. **44**, 1 (1991).
[2] L. P. Kouwenhoven, Science **275**, 1896 (1997).
[3] A. Aviram and M. A. Ratner, Chem. Phys. Lett. **29**, 277 (1974); *Molecular Electronics—Science and Technology*, AIP Conference Proceedings No. 262, edited by A. Aviram (AIP, New York, 1992).
[4] W. P. Su, J. R. Schrieffer, and A. J. Heeger, Phys. Rev. Lett. **42**, 1698 (1979); C. Joachim and J. F. Vinuesa, Europhys. Lett. **33**, 635 (1996); M. P. Samanta, W. Tian, and S. Datta, Phys. Rev. B **53**, R7626 (1996); V. Mujica, M. Kemp, and M. A. Ratner, J. Chem. Phys. **101**, 6849 (1994).
[5] D. M. de Leeuw, Synth. Met. **55–57**, 3597 (1993); P. Bäuerle, T. Fischer, B. Bidlingmeier, A. Stabel, and J. P. Rabe, Angew. Chem. Int. Ed. Engl. **34**, 303 (1995); J. M. Tour, Chem. Rev. **96**, 537 (1996).
[6] G. Schmid, *Clusters and Colloids. From Theory to Applications* (VCH, Weinheim, 1994); *Physics and Chemistry of Metal Cluster Compounds*, edited by L. de Jongh (Kluwer, Dordrecht, 1994); Y. Volokitin, J. Sinzig, L. J. de Jongh, G. Schmid, and I. I. Moiseev, Nature (London) **384**, 621 (1996).
[7] D. C. Ralph, C. T. Black, and M. Tinkham, Phys. Rev. Lett. **74**, 3241 (1995).
[8] D. L. Klein and P. L. McEuen, Appl. Phys. Lett. **68**, 1 (1996).
[9] M. A. Reed, C. Zhou, C. J. Muller, T. P. Burgin, and J. M. Tour (unpublished).
[10] A. Korotkov and Yu. Nazarov, Physica B **173**, 217 (1991).
[11] R. Stratton, J. Phys. Chem. Solids **23**, 1177 (1962).
[12] A. Bezryadin and C. Dekker, J. Vac. Sci. Technol. B **15**, 793 (1997).